Amino Acid Substitution at Position 99 Affects the Rate of CRP Subunit Exchange†

Cheryl H. Baker,‡ Steven R. Tomlinson,§ Angel E. García,|| and James G. Harman*,§

Theoretical Biology and Biophysics, Group T10, Mail Stop K710, Los Alamos National Laboratory, Los Alamos, New Mexico 87545, and Department of Chemistry and Biochemistry, Texas Tech University, Lubbock, Texas 79409-1061

Received April 24, 2001; Revised Manuscript Received June 27, 2001

ABSTRACT: We investigated the characteristics of CRP having amino acid substitutions at position 99. Analysis of amino acid residue proximity to cAMP in molecular dynamics (MD) simulations of the CRP:$(cAMP)_2$ complex [García, A. E., and Harman, J. G. (1996) *Protein Sci. 5*, 62−71] showed repositioning of tyrosine 99 (Y99) to interact with the equatorial exocyclic oxygen atom of cAMP. To test the role of Y99 in cAMP-mediated CRP activation, Y99 was substituted with alanine (A) or phenylalanine (F). Cells that contained the WT or mutant forms of CRP induced β-galactosidase in the presence of cAMP. Purified WT, Y99A, and Y99F CRP showed only a 3- to 4-fold difference in cAMP affinity. There were no apparent differences between the three forms of CRP in cAMP binding cooperativity, in CRP:$(cAMP)_1$ complex binding to *lac*P DNA, in the formation of CRP:cAMP:RNAP complexes at *lac*P, or in CRP efficacy in mediating *lac*P activity in vitro. The apo-form of Y99A CRP was more sensitive to protease than the apo-form of either WT CRP or Y99F CRP. Whereas the WT or Y99F CRP:$(cAMP)_1$ complexes were cleaved by protease at hinge-region peptide bonds, the Y99A CRP:$(cAMP)_1$ complex was cleaved at peptide bonds located at the subunit interface. The rates of subunit exchange for Y99A CRP, both in the apo-form and in a 1:1 complex with cAMP, were significantly greater than that measured for WT CRP. The results of this study show that tyrosine 99 contributes significant structural stability to the CRP dimer, specifically in stabilizing subunit association.

Cyclic 3′:5′-adenosine monophosphate (cAMP)[1] plays an important role in regulating the activity of several catabolic genes in *Escherichia coli*. The effects of cAMP are mediated through its binding to the cAMP receptor protein (CRP) (*1*). CRP is a 47 238 Da dimer composed of two identical 209-amino acid subunits, each of which can bind cAMP (*2*−*4*). Three cAMP-dependent forms of CRP are known; apo-CRP, CRP:$(cAMP)_1$, and CRP:$(cAMP)_2$ (*5*, *6*). At micromolar concentrations, cAMP binding produces conformational changes in CRP that result in a modest increase in CRP subunit stability, affect the susceptibility of CRP hinge region peptide bonds to protease, introduce CRP site-specific DNA binding and promote CRP interaction with RNA polymerase (RNAP) (*7*−*12*).

CRP:$(cAMP)_2$ structure has been determined to 2.5 Å resolution (i.e., 3GAP) and, more recently, to 2.1 Å resolution (i.e., 1G6N) from the analysis of X-ray data derived from CRP crystals grown in the presence of cAMP (*4*, *13*). Each CRP subunit folds into two domains. The large amino-proximal domain contains extensive β-sheet structure which forms the cAMP binding pocket, and three α-helices (designated A, B, and C). The smaller carboxyl-proximal domain is composed principally of three α-helices (designated D, E, and F) two of which, the E and F helices, form the DNA binding surface of CRP. The structural changes induced in CRP upon binding cAMP include changes in the cyclic nucleotide-binding domain, the DNA binding domain, the interdomain hinge-region and in regions involved in CRP intersubunit interaction (*14*−*16*).

From the analysis of CRP:$(cAMP)_2$ structure, Weber and Steitz (*4*) identified five amino acid−ligand contacts that were likely to be important in cAMP binding to CRP in solution and/or in mediating cAMP activation of CRP. The charged phosphate of cAMP aligns with arginine (R) 82 to form a salt bridge. Specific hydrogen-bonding interactions occur between the axial exocyclic oxygen atom of cAMP and serine (S) 83, the ribose 2′ hydroxyl and glutamate (E) 72, and the adenine N^6 amino group and threonine (T) 127 of one subunit and S128 of the other subunit. They also proposed that tyrosine (Y) 99 played a role in stabilizing the cAMP binding pocket through hydrogen-bonding interactions with both the carbonyl oxygen of glycine (G) 71 and R82 (*4*).

One characteristic of both 3GAP and 1G6N is CRP subunit asymmetry with one subunit adopting an open conformation and the other subunit adopting a closed conformation (*4*, *13*).

† This work was funded through the Robert A. Welch Foundation (Grant D-1248), the Los Alamos National Laboratory LDRD Program (Award 96013), and seed grants from the Texas Tech University Graduate School and the Texas Tech University Institute for Biotechnology.

* To whom correspondence should be addressed. Phone: (806) 742-1297. Fax: (806) 742-1289.

‡ Current address: Department of Cancer Biology, MD Anderson Cancer Center, 1515 Holcombe Boulevard, Houston, Texas 77030.

§ Department of Chemistry and Biochemistry.

|| Theoretical Biology and Biophysics.

[1] Abbreviations: cyclic AMP or cAMP, cyclic 3′:5′-adenosine monophosphate; CRP, cAMP receptor protein; MD, molecular dynamics; *lac*P, lactose operon promoter; RNAP, RNA polymerase; ANS, 8-anilino-1-naphthalenesulfonic acid; MALDI-TOF MS, matrix-assisted laser desorption/ionization time of flight mass spectrometry.

10.1021/bi010834+ CCC: $20.00
Published on Web 09/22/2001

Table 1: Oligonucleotide Sequences Used for *crp* Mutagenesis

designation	oligonucleotide sequence
Y99A-1	pGAAATTTCGGCCAAAAAATTT
Y99F-1	pGAAATTTCGTTCAAAAAATTT
T127C	pCGTCGTTCTGCAAGTCTGTTCAGAGAAAGTGGGCAAC
T127C-rc	pGTTGCCCACTTTCTCTGAACAGACTTGCAGAACGACG
CRP stop	pCGGCACTCGTAGATCTTAGCACCATCACCATCACTAA
CRP stop-rc	pTTAGTGATGGTGATGGTGCTAAGATCTACGAGTGCCG
Y99A-2	pGCTGAAATTTCGTTCAAAAAATTTCGC
Y99A-2rc	pGCGAAATTTTTTGAACGAAATTTCAGC
Y99F-2	pGCTGAAATTTCGGCCAAAAAATTTCGC
Y99F-2rc	pGCGAAATTTTTTGGCCGAAATTTCAGC
LCAP	pGCAACGCAATTAATGTGAGTTAGCTCACTCATTAGGCACCC
LCAP-rc	pGGGTGCCTAATGAGTGAGCTAACTCACATTAATTGCGTTG
LRAN	pGCAACGCAATACATCTGGATGTACAATAAGTGTAGGCACCC
LRAN-rc	pGGGGTGCCTACACTTATTGTACATCCAGATGTATTGCGTTG

Molecular dynamics (MD) simulation studies conducted using 3GAP as the initial structure predicted the transition of CRP:$(cAMP)_2$ from an open/closed subunit configuration to a closed/closed configuration similar to that observed in CRP:$(cAMP)_2$:DNA crystals (*17*, *18*). Analysis of the conformations sampled during the MD simulations showed that CRP:cAMP contacts in the initial structure were maintained and, in addition, a new contact was established involving the interaction of tyrosine at position 99 (Y99) and cAMP bound to the B subunit of CRP. To test the presence and significance of this Y99:cAMP interaction on CRP function, the *crp* gene was mutated to replace Y99 with either alanine (A) or phenylalanine (F). The results of this study show that the amino acid residue at position 99 plays an important role in determining the strength and stability of CRP subunit interactions. In addition, we present evidence for two protease targets in CRP: one that lies in the hinge region and a second that lies along the C-helix. Peptide bonds in the CRP hinge are accessible to protease in the CRP:cAMP complex, while those located along the C-helix are accessible to protease in the apo-CRP monomer.

MATERIALS AND METHODS

Molecular Dynamics Simulations. In vacuo (625 ps) and solution (140 ps) molecular dynamics simulations using the CRP:$(cAMP)_2$ structure of Weber and Steitz (*4*) (accession # 3-GAP) as the initial structure were reported earlier (*17*). Principle component analysis was used to track large amplitude global conformational changes in CRP conformation during the course of simulation (*19*, *20*).

Bacterial Strains and Plasmids. *E. coli* CA8445/pRK248 (*21*), M15/pREP4 (*14*), and MZ-1 (*22*) were used as host strains for recombinant *crp* plasmids. Plasmid pRK248 (λcI^{ts}, tet^r) (*23*) encodes a thermolabile λcI repressor used to control the λP_L promoter. Plasmid pREP4 encodes the Lac repressor used to control CRP synthesis that originates from *lac*P (*14*). Plasmids pHA7 (*3*) and pQE60NB1 (*14*) encode, respectively, WT CRP expressed from *tet*P and MVRRASV-CRP-RSH_6 CRP expressed from *lac*P. Plasmid pLEX (Invitrogen) was used for high-level Y99A and Y99F CRP expression. Plasmid pKL201 (*21*) was used as the *lac*P template for in vitro transcription studies. Derivatives of M13/*crp Nde*I (*24*) were grown on *E. coli* strain XL-1 Blue (Stratagene). *E. coli* strains MV1190 and CJ236 (Bio-Rad) were used for mutagenesis of *crp*. RNA polymerase was purified from *E. coli* strain AG1 (Stratagene).

Enzymes and Other Materials. Restriction enzymes were obtained from New England Biolabs. Shrimp alkaline phosphatase, phenylmethylsulfonyl fluoride (PMSF), and isopropylthio-β-D-galactopyranoside (IPTG) were purchased from United States Biochemical Corporation. Nucleoside triphosphates and 1 mL of HiTrap Ni-chelating columns were purchased from Pharmacia. X-ray film (BMX-2) was purchased from Eastman Kodak. [α-^{32}P]UTP and [γ-^{32}P]ATP were purchased from New England Nuclear. Cyclic AMP, subtilisin BPN′ (type XXVII, 7.9 units/mg) and the catalytic subunit of bovine heart cAMP-dependent protein kinase was purchased from Sigma Chemical Co. Econo-Pac ion exchange cartridges, precast 10−20% polyacrylamide gels, and Mutagene M13 in vitro mutagenesis kits were purchased from Bio-Rad Laboratories. DNA isolation kits were purchased from Qiagen and from Promega. Synthetic oligonucleotides were synthesized by the Texas Tech University Biotechnology Institute Core Facility. Common salts and buffers were reagent grade or better.

Site-Directed Mutagenesis of crp. Amino acid substitution of CRP was accomplished by the method of Kunkel (*25*) using M13/*crp Nde*I (*24*) vector DNA as template. Single-stranded primers were used to substitute an alanine (Y99A-1) or a phenylalanine (Y99F-1) codon for the tyrosine 99 codon (Table 1). The 1.5 Kbp *Pvu*II DNA fragment of mutagenized M13/*crp Nde*I RF DNA was subcloned into *Pvu*II-digested, alkaline phosphatase-treated pLEX vector DNA. Plasmid DNA was purified and analyzed by *Nde*I digestion to establish the orientation of the cloned *crp* genes. *Nde*I-digested plasmid DNA that contained either the *crp*99A or the *crp*99F allele in the correct orientation was diluted and ligated to position the *crp* initiation codon proximal to the pLEX λcII ribosome binding site. DNA sequence analysis of the *crp* gene was performed to confirm the plasmid constructs.

Double-stranded plasmid DNA mutagenesis was accomplished using the Quick-Change PCR protocol (Stratagene). The T127C amino acid substitution was introduced into plasmid pLEX *crp*Y99A using the mutagenic oligonuceotide pair T127C/T127C-rc (Table 1). Plasmid pQE60NB1$_\Delta H_6$, a pQE60NB1 derivative having a translation stop codon immediately upstream of the hexahistidine codons, was constructed using the oligonuceotide pair CRP stop/CRP stop-rc (Table 1). Mutagenic oligonucleotide pairs used to introduce alanine or phenylalanine codons at position 99 in the *crp* contained in plasmids pQE60NB1, pQE60NB1$_\Delta H_6$,

and pHA7 were Y99A-2/Y99A-2rc and Y99F-2/Y99F-2rc (Table 1).

Assay of β-Galactosidase. CA8445/pRK248 cells harboring pHA7, pHA7 *crp*Y99A, or pHA7 *crp*Y99F were cultured as described by Belduz et al. (*24*). Samples were assayed for β-galactosidase activity according to Miller (*26*).

Proteins. *(a) CRP Isolation*. The Y99A, Y99F, and Y99A/T127C CRP were prepared using standard ion-exchange chromatography techniques. CRP induction was carried out as described previously (*21*). Frozen cell pellets were thawed and suspended in 20 mL of ice-cold 25 mM sodium phosphate, pH 7.2, that was 1 mM in EDTA, 1 mM in β-mercaptoethanol, and 5% (v/v) in glycerol (NP buffer), and the cells were ruptured with two passages through a French pressure cell at 500 psi. The suspension was clarified by centrifugation, and the soluble protein fraction was dialyzed overnight against NP buffer. Extracts were applied to an Econo-Pac ion exchange High Q cartridge (Bio-Rad) connected in tandem to a Econo-Pac ion exchange High S cartridge (Bio-Rad) and washed with NP buffer until the eluate $A_{280} < 0.1$. The anion-exchange column was removed, and CRP was eluted from the cation exchange column in a linear salt gradient prepared from 100 mL of NP buffer and 100 mL of NP buffer that was 0.3 M in NaCl. Protein fractionation was monitored by sample A_{280}, and samples were analyzed on polyacrylamide−SDS gels stained with acidic coomassie blue. Fractions that contained CRP at high concentration and purity were pooled and dialyzed against NP buffer that was 100 mM in NaCl. CRP was judged to be greater than 97% homogeneous for the WT preparation and greater than 94% homogeneous for the Y99A, Y99F, and Y99A/T127C CRP preparations. CRP concentrations were determined using an extinction coefficient of 3.5×10^4 M^{-1} cm^{-1} at A_{279}. *(b) MVRRASV-CRP-RSH$_6$ and MVRRASV-CRP-RS Isolation*. The plasmids pQE60NB1 and pQE60NB1$_\Delta$H$_6$ were transformed into *E. coli* strain M15/pREP4. *MVRRASV-CRP-RSH$_6$* and *MVRRASV-CRP-RS* synthesis was induced as described by Baichoo and Heyduk (*14*). Cells were harvested by centrifugation and stored at −80 °C. *E. coli* M15/pREP4/pQE60NB1 cells were thawed on ice and suspended in ice-cold buffer that was 25 mM in sodium phosphate, pH 7.4, and 100 mM in imidazole. The cells were ruptured in a French pressure cell and the suspension was clarified at 4 °C by centrifugation. The clarified extracts were filtered through 0.45 μm Millipore filters and *MVRRASV-CRP-RSH$_6$* was purified over a Ni-chelating column. *E. coli* M15/pREP4/pQE60NB1$_\Delta$H$_6$ cell pellets were suspended in NP buffer, and the cell extracts were prepared as described above. The *MVRRASV-CRP-RS* contained in these extracts was purified over BioRex 70 resin as described by Harman et al. (*21*). *(c) RNA Polymerase Isolation*. RNA polymerase was isolated as described previously (*27*, *28*).

Protease Probe of CRP Structure. Protease digestion reactions were run at 23 °C in a volume of 40 μL in NP buffer that was 100 mM in NaCl (*6*). Reaction mixtures contained 20 μg of CRP and, where indicated, cAMP. Peptides were resolved on 10 to 20% gradient polyacrylamide−SDS gels, visualized by staining with acidic coomassie blue R-250, and quantitated using a Molecular Dynamics 300B laser densitometer. Samples were prepared for N-terminal amino acid sequence analysis by equilibrating the gels in a 10 mM in CAPS buffer (pH 11) solution that was 10% in methanol and 2 mg/mL in dithiothreitol. The peptides were electrophoretically transferred to a PVDF membrane. PVDF membranes were stained for 1 min in a 0.1% solution of coomassie blue R-250, 40% in methanol and1% in acetic acid and destained in 50% methanol solution. The CRP core fragments were excised and analyzed in a Porton model 2020 peptide sequencer.

CRP Core Fragment Mass Determinations. A total of 50 μg of WT, Y99A, and T127C/Y99A CRP were digested with subtilisin as described above. The reaction mixtures were absorbed to DE81 ion exchange filters (Whatman) that had been equilibrated in NP buffer lacking β-mercaptoethanol. The core fragments were eluted in 300 μL of water and dialyzed against 1000 vol of water for 6 h at 4 °C. The samples were dried in vacuo, dissolved in 20 μL water and diluted with 2 vol of ionizing matrix solution that was 10 mg/mL in sinapinic acid, 10% in trifluoroacetic acid, and 50% in acetonitrile. The samples were analyzed on a PerSeptive Biosystem Voyager DE matrix-assisted laser desorption/ionization time-of-flight mass spectrometer (MALDI-TOF MS). Spectra were calibrated to cytochrome C and lysozyme.

Cyclic AMP Binding Assay. Fluorescence titration experiments were conducted at room temperature on protein samples that had been dialyzed against 50 mM Tris-HCl (pH 7.8), 0.1 M KCl, and 1 mM EDTA. Fluorescence measurements were performed and the data were analyzed as previously described (*29*).

DNA Binding Assay. Two 41 bp double-stranded DNA fragments were utilized in the DNA binding assay. One fragment, LCAP contained a binding site for CRP was prepared by annealing oligonucleotide pairs LCAP/LCAP-rc (Table 1) as described (*10*). The second fragment, LRAN, lacking a CRP binding site was prepared by annealing oligonucleotide pairs LRAN/LRAN-rc (Table 1) as described (*10*). Binding reactions were run in transcription buffer [30 mM in Tris-HCl (pH 8.0), 2.5 mM in $MgCl_2$, 0.1 mM in EDTA, 0.1 mM in DTT, 100 mM in KCl] that contained 5 μg/mL BSA with duplex DNA at 27 pM, CRP at the indicated concentration, and when present, cAMP at 200 μM. The data were analyzed as described previously (*29*).

In Vitro DNase I Footprinting and Transcription Assays. DNase I footprinting reactions and transcription reactions were carried out as described previously (*29*).

Subunit Exchange Reactions. *MVRRASV-CRP-RS Labeling*. The MVRRASV-CRP-RS at 1 mg/mL was labeled in an 80 μL reaction that contained 18.8 units of bovine heart muscle cAMP-dependent protein kinase catalytic subunit and was 0.2 μM in [γ-^{32}P]ATP as described by Baichoo and Heyduk (*14*). The reaction mixture was loaded onto BioRex 70 resin and washed with 20 mM sodium phosphate, pH 7.2, that was 50 mM in NaCl to remove unincorporated label. Radiolabeled MVRRASV-CRP-RS was eluted from the column in 20 mM sodium phosphate, pH 7.2, that was 600 mM in NaCl. Fractions containing radiolabeled MVRRASV-CRP-RS were pooled and stored at −20 °C.

Subunit exchange was performed in buffer that was 25 mM in sodium phosphate (pH 7.2), 100 mM in NaCl, 5% (v/v) in glycerol, 0.01% (w/v) in sodium azide, and, where indicated, contained cAMP. The total CRP concentration used in these experiments was 2.7 μg/mL; MVRRASV-CRP-

RSH_6 and radiolabeled MVRRASV-CRP-RS were mixed at a ratio of 9:1. The assay was initiated by equilibrating the radiolabeled MVRRASV-CRP-RS in subunit exchange buffer for 12 h at room temperature. Subunit exchange was initiated by adding unlabeled MVRRASV-CRP-RSH_6, and the reaction mixture was incubated at 26 °C. At different time intervals, 1.0 mL of exchange solution was loaded onto a Ni-chelating column. The column was washed with 4.0 mL of wash buffer [20 mM sodium phosphate, pH 7.2; 300 mM NaCl; 100 mM imidazole] followed by 4.0 mL of elution buffer [20 mM sodium phosphate, pH 7.2; 500 mM NaCl; 500 mM imidazole]. The column load, wash and elution steps took, on average, 3 min. The radioactivity contained in the wash and elution samples was determined using standard scintillation techniques. Control experiments showed that 96% (±1.5%) of labeled MVRRASV-CRP-RSH_6 applied to the column was bound by and eluted from the column under the conditions outlined above. Nonspecific binding of radiolabled MVRRASV-CRP-RS averaged 15.0% (±5%) and was evident in the time = 0 (T_0) samples. The amount of radiolabled MVRRASV-CRP-RS specifically bound to the column through association with MVRRASV-CRP-RSH_6 for a given time (T_N) during exchange was calculated using the relationship: % bound = [(T_n elution counts − T_0 elution counts)/total counts] × 100.

RESULTS

In 3GAP, Y99 occupies the N-terminal position of the CRP B helix with the bulk of the side chains buried and the hydroxyl groups directed toward cAMP (Figure 1). At 4.6 Å (subunit A) and 4.2 Å (subunit B), the Y99 hydroxyl groups are sufficiently far to preclude prediction of a direct interaction between Y99 and cAMP. Weber and Steitz (*4*) did, however, predict that the residues forming the cAMP pocket were stabilized by Y99 hydrogen bonding to R82 and the carbonyl oxygen of G71. We have previously reported on molecular dynamics (MD) simulations of the CRP:$(cAMP)_2$ complex using 3GAP as the initial structure (*17*). These simulations predict that when removed from the crystalline environment CRP:$(cAMP)_2$ structure undergoes a transition from the open:closed subunit configuration to a closed:closed subunit configuration observed for the CRP:$(cAMP)_4$:DNA complex (*17*, *18*). Much of the difference between the crystalline and noncrystalline structures resulted from concerted, time-dependent, C-terminal domain motion in the B subunit (*17*). Analysis of the CRP:$(cAMP)_2$ structures sampled throughout the MD simulations showed Y99 of subunit B to reposition to allow direct hydrogen bonding between the Y99 hydroxyl and cAMP bound to the B subunit (data not shown). The geometry of this interaction was such that Y99 hydrogen bonded with both the equatorial exocyclic oxygen atom of cAMP and the guanidinium of R82. Two separate 29 picosecond (ps) MD simulations of solvated CRP:$(cAMP)_2$ reproduced the Y99 movement to interact with cAMP within the first picosecond of each simulation. This interaction was maintained for 10 ps in one simulation and for 29 ps in a second simulation. The results of the short, nonequilibrium, MD simulations indicated that, upon removal of crystal lattice constraints, Y99 repositioning to interact with cAMP was reproducible. More extensive 2.6 ns MD simulations of CRP:$(cAMP)_2$ in aqueous solution

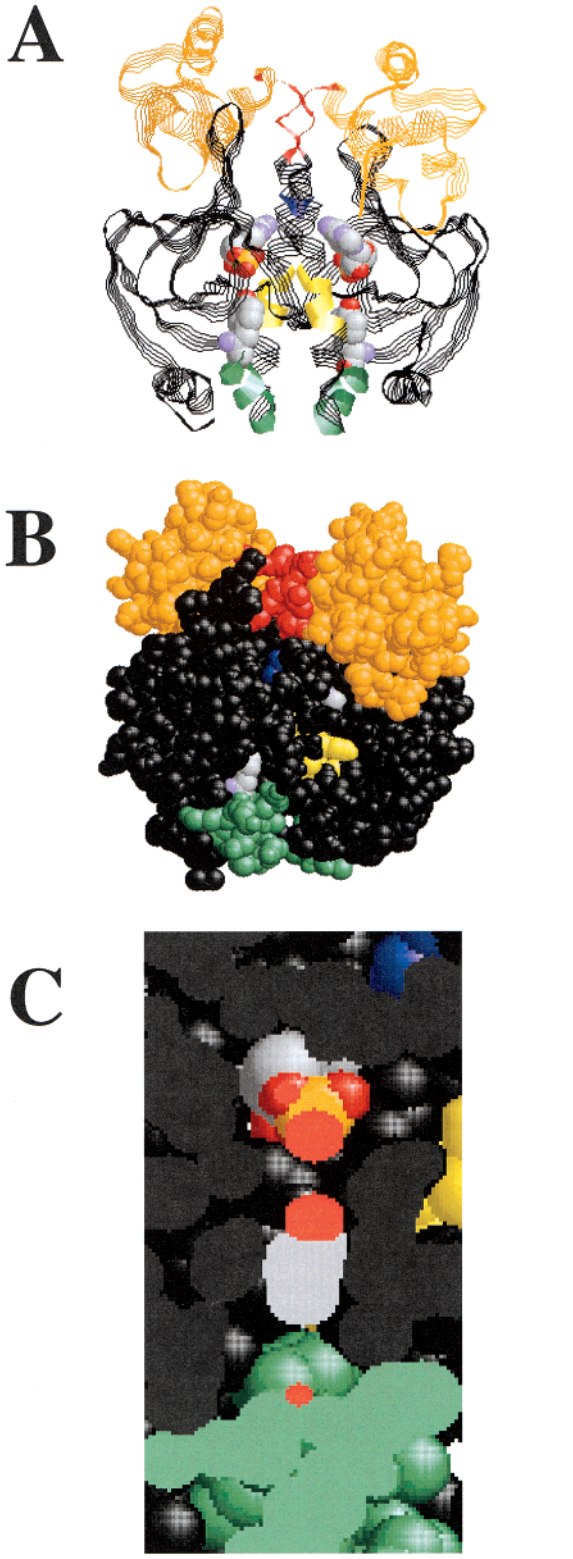

FIGURE 1: CRP:$(cAMP)_2$ dimer structure. Panel A shows the CRP dimer presented as a strand model, cAMP and Y99 are space-filled and presented in CPK colors. Panel B shows the CRP dimer presented as a space-filled model. For both panel A and panel B, the N-proximal cAMP binding domains (residues 1−133) are black, the C-proximal DNA binding domains (residues 140−209) are gold. The hinge-region connecting the two domains is red. The B-helix is presented as green ribbon. The C-helix region L116 through A121 is yellow ribbon and S128 is blue ribbon. Panel C shows the Y99 region of the space filled CRP structure presented in slab-mode. Figures were generated from the 3GAP coordinates (*4*) using RasMac ver. 2.7.1.

Table 2: Summary of Binding Properties for the WT, Y99A, and Y99F CRP[a]

	K_{app}^{LCAP} (M^{-1})	K_{app}^{LCAP} (M^{-1})	K_{app}^{LRAN} (M^{-1})	K_{app}^{cAMP1} (M^{-1})	K_{app}^{cAMP2} (M^{-1})
CRP	no cAMP	200 μM cAMP	200 μM cAMP		
WT	$(1.3 \pm 3.9) \times 10^5$	$(2.5 \pm 1.1) \times 10^7$	$(3.8 \pm 1.1) \times 10^5$	$(3.3 \pm 1.3) \times 10^5$	$(1.8 \pm 3.9) \times 10^2$
A	$(1.5 \pm 3.9) \times 10^5$	$(2.8 \pm 0.3) \times 10^7$	$(7.2 \pm 2.9) \times 10^5$	$(1.3 \pm 0.8) \times 10^6$	$(3.9 \pm 2.6) \times 10^2$
F	$(1.7 \pm 0.4) \times 10^5$	$(2.5 \pm 0.3) \times 10^7$	$(3.3 \pm 0.1) \times 10^5$	$(6.7 \pm 1.5) \times 10^5$	$(3.3 \pm 0.8) \times 10^2$

[a] Apparent association constants K_{app}^{LCAP}, K_{app}^{LRAN}, K_{app}^{cAMP1}, and K_{app}^{cAMP2} were determined from fits of the data presented in Figure 3 and Figure 4, respectively, as described in ref *29*. Errors are expressed as 1 SD.

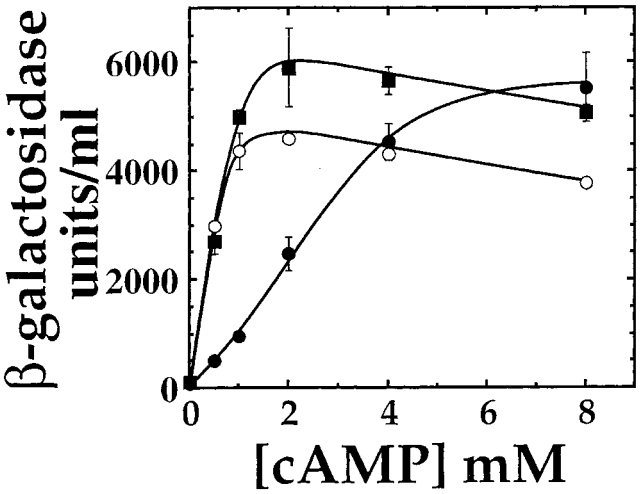

FIGURE 2: β-Galactosidase activity in cells containing the WT or position 99 mutant forms of CRP. CRP was expressed in *E. coli* strain CA8445/pRK248. Each value is the mean of at least two independent experiments. WT CRP (open circles); Y99A CRP (closed circles); Y99F CRP (closed squares). The basal levels of β-galactosidase measured in the absence of added cAMP were 93, 107, and 97 units/ml for cells containing the WT, Y99A, and Y99F CRP, respectively.

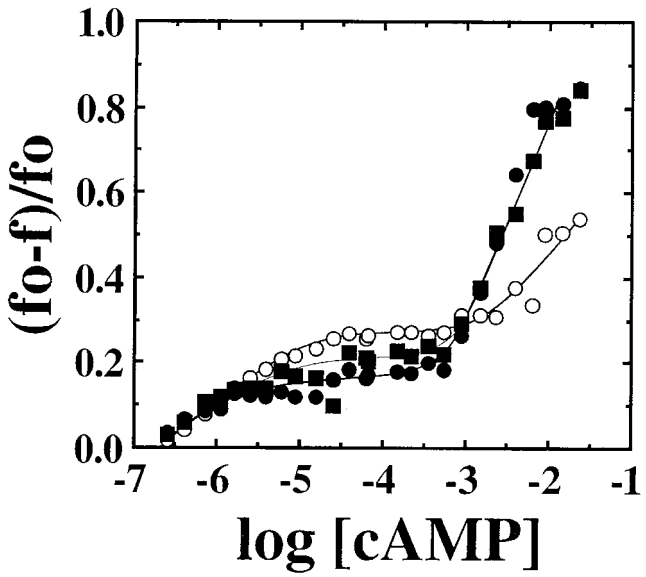

FIGURE 3: Binding of cAMP to CRP. The fluorescence of WT (open circles), Y99A (closed circles), and Y99F CRP (closed boxes) ANS−CRP complexes measured as a function of cAMP concentration. The data were fit as described in ref *29*. Each data point is the average of at least two experiments.

suggest that Y99 may form a water-mediated contact with cAMP (García and Harman, unpublished material).

To determine the significance of this putative Y99−cAMP interaction, we have examined the effects of position 99 amino acid substitutions on CRP structure and function. To this end, in vivo experiments were conducted to assess CRP-mediated induction of β-galactosidase activity in cells that contained either pHA7 (encoding WT CRP), pHA7*crp*99A (encoding Y99A CRP), or pHA7*crp*99F (encoding Y99F CRP). Data presented in Figure 2 illustrate that each cell type produced a basal level of β-galactosidase in the absence of cAMP and increased β-galactosidase activity in response to cAMP addition to the culture medium. For the WT CRP and Y99F CRP, β-galactosidase activity peaked between 1.0 and 2.0 mM cAMP, whereas for the Y99A CRP, β-galactosidase activity peaked at a cAMP concentration of 8.0 mM. For reasons that are not clear to us, cells that contained the Y99A and Y99F CRP consistently produced 25% higher levels of β-galactosidase than cells that contained WT CRP (Figure 2). The results of the in vivo studies show that substitution of Y99 by alanine affects CRP efficacy in promoting *lac* mRNA synthesis, effects manifest on the concentration of ligand required for maximum activity.

The WT and position 99 mutant forms of CRP were purified and characterized in vitro. To assess cAMP binding, fluorescence changes resulting from cAMP titration of ANS−CRP complexes were measured and analyzed (Figure 3, Table 2). The apparent association constants, K_{app}^{cAMP1}, for all three proteins were in the range of 3×10^5 to 13×10^5 M^{-1}. The calculated values for K_{app}^{cAMP2} were on the order of 3×10^2 M^{-1} (Figure 3, Table 2). From this we conclude that negative cooperativity in cAMP binding, a characteristic of WT CRP, is also characteristic of the Y99A and Y99F forms of CRP.

In the absence of cAMP, the WT, Y99A and Y99F forms of CRP bound DNA that contained a CRP binding site (LCAP) with low affinity having apparent association constant values, K_{app}^{DNA}, that ranged from 1.3×10^5 to 1.7×10^5 M^{-1} (Figure 4, Table 2). Each CRP bound, in the presence of cAMP, a DNA fragment that did not contain a CRP binding site (LRAN) with similarly low affinity having K_{app}^{DNA} values that ranged from 3.8×10^5 to 7.2×10^5 M^{-1}. All three proteins complexed with cAMP bound LCAP DNA with 150−200-fold greater affinity than the apo-forms having K_{app}^{DNA} values of 2.5×10^7, 2.8×10^7, and 2.5×10^7 M^{-1} for the WT, Y99A, and Y99F CRP, respectively. Cyclic AMP binding induced in all three forms of CRP a conformation change that lead to site-specific DNA binding. Indeed, the DNase I footprints of *lac*P were equivalent for each CRP:$(cAMP)_1$ complex (data not shown). Furthermore, each CRP:$(cAMP)_1$ complex promoted RNAP binding and DNase I footprinting of LCAP DNA. The results of both the cAMP and the DNA binding studies show that amino acid substitution at position 99 has little effect on the ligand binding characteristics of CRP.

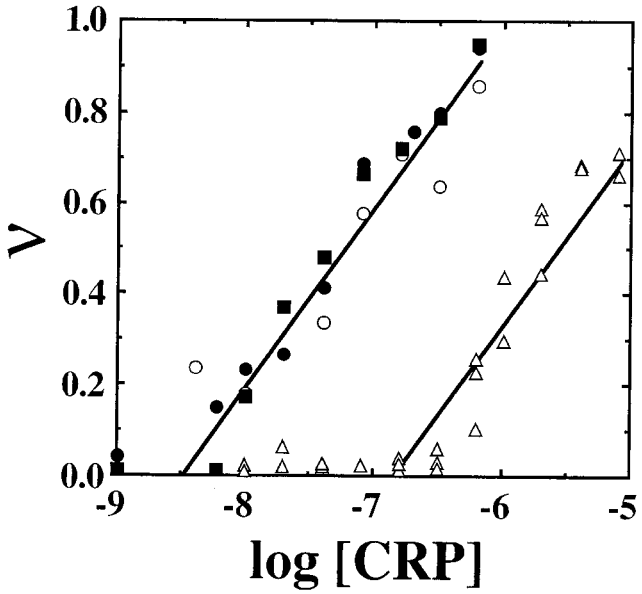

FIGURE 4: Binding CRP to DNA. Reactions contained either WT CRP (open circles), Y99A CRP (closed circles), or Y99F CRP (closed boxes) at the indicated concentrations, LCAP or LRAN at 27 pM, and when present, cAMP at 200 μM. The data were fit as described in ref *29*. The data from reactions run on LCAP DNA the absence of cAMP, and on LRAN DNA in the presence of cAMP are represented by open triangles.

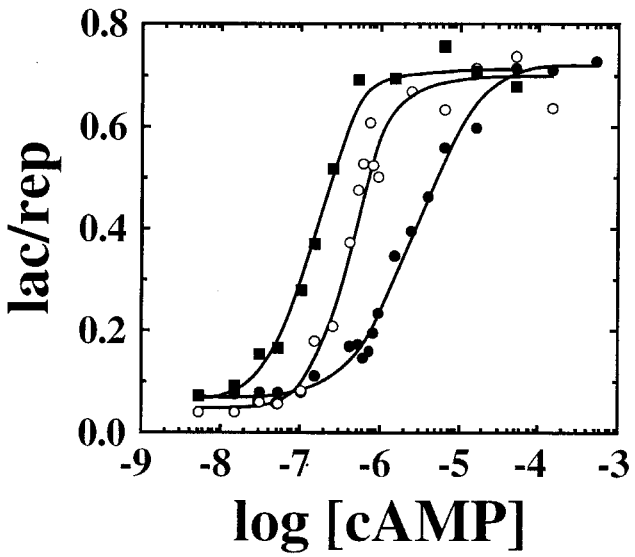

FIGURE 5: Effect of cAMP on l*ac* transcription promoted by the WT CRP (open circles), Y99A CRP (closed circles), or Y99F (closed boxes). Reaction mixtures contained supercoiled template DNA, RNAP, CRP and the indicated concentrations of cAMP. Autoradiographs of the RNA products separated on 6% polyacrylamide gels 7 M in urea were scanned on a laser densitometer and the *lac* and *rep* RNA bands quantitated.

To evaluate the efficacy of the ternary complexes formed at *lac*P containing either WT or mutant forms of CRP:cAMP complex, we quantitated the amount of *lac* RNA synthesized from *lac* in reaction mixtures that contained either the WT CRP, Y99A CRP, or Y99F CRP (Figure 5). In these reactions, the *rep* transcript originating from the CRP-independent *rep* promoter served to normalize individual reactions in a reaction series and to normalize reaction series conducted using different CRP preparations. Similar to the results obtained in vivo, neither the WT CRP nor the mutant forms of CRP supported significant levels of *lac*P mRNA

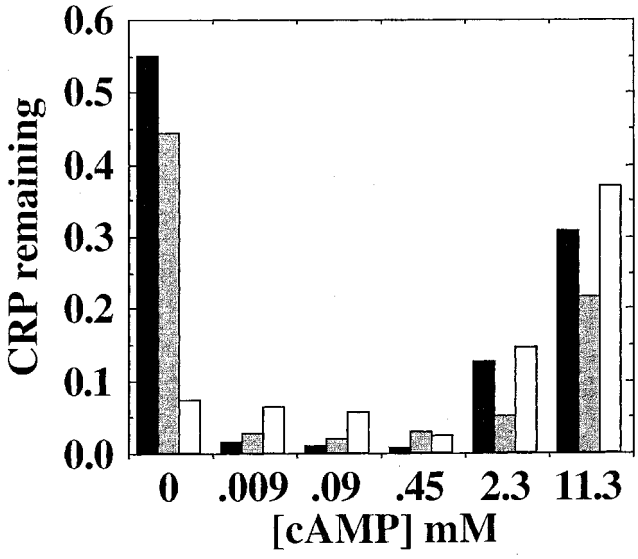

FIGURE 6: Protease sensitivity of WT or position 99 mutant forms of CRP. CRP was incubated with subtilisin in the presence or absence of cAMP. Samples were separated on 10−20% SDS−PAGE gels and the amount of intact CRP remaining was determined. The histogram displays the fraction of intact monomer remaining for WT (black bars), Y99F (striped bars), and Y99A (white bars) at the indicated concentrations. Data are from a single protease reaction series and are representative results.

synthesis in vitro in the absence of cAMP. In the presence of cAMP at concentrations greater than 50 μM, reaction mixtures that contained any one of the three forms of CRP showed high-level *lac* mRNA synthesis. The concentration of cAMP required for half-maximal *lac* RNA synthesis was different for each of the three proteins. The concentration of cAMP required for half-maximal *lac* mRNA synthesis in transcription reactions that contained the WT CRP, Y99A CRP or Y99F CRP was 0.3, 2.0, and 0.13 μM, respectively.

Cyclic AMP binding studies coupled with CRP structure analysis have shown that three cAMP-dependent CRP conformers exist: that of apo-CRP, that of the CRP:$(cAMP)_1$ complex having one cAMP binding site occupied, and that of the CRP:$(cAMP)_2$ complex having both cAMP binding sites occupied (*7*, *8*). These CRP conformers are distinguished in their sensitivity to protease (*8*). Apo-CRP has a protease-resistant hinge whereas CRP:$(cAMP)_1$ and CRP:$(cAMP)_2$ have protease-sensitive hinges with CRP:$(cAMP)_1$ being digested more rapidly than CRP:$(cAMP)_2$.

The results of protease digestion assays show that amino acid substitution at position 99 produced clear effects on CRP structure (Figure 6). In the apo-form, WT CRP and Y99F CRP were relatively resistant to subtilisin, whereas the Y99A CRP was degraded by the subtilisin. At micromolar cAMP concentrations, all three proteins were protease sensitive and at millimolar cAMP concentrations the protease sensitivity exhibited by all three proteins decreased. Subtilisin generated a low-mass core fragment population from the Y99A CRP in reaction mixtures that contained between 9 and 90 μM cAMP. In contrast, subtilisin generated high-mass core fragment populations in reaction mixtures that contained either WT CRP or Y99F CRP and 9 μM to 20 mM cAMP or in reaction mixtures that contained Y99A CRP and 20 mM cAMP. N-Terminal amino acid sequence analysis showed that all of the CRP core populations contained two predominant N-terminal amino acid sequences (Table 3). One

Table 3: Summary of N-Terminal Amino Acid and MALDI-TOF Mass Spectral Analysis of the WT, Y99A, Y99A/T127C, and Y99F α-Core Fragments

CRP	N-terminal sequence	MALDI-TOF mass	predicted masses	predicted sequence
WT (90 μM)	VL/GKPQTD	15 050	15 055	G4−L134
		15 264	15 267	V2−L134
Y99A (90 μM)	VL/GKPQTD	13 008	12 992	G4−L116
		13 091	13 079	G4−L117
		13 297	13 292	V2−L117
		13 497	13 481 or	G4−A121
			13 491	V2−Q119
Y99A (20 mM)	VL/GKPQTD	14 313	14 322	G4−S128
Y99A/T127C (90 μM)	VL/GKPQTD	14 310	14 324	G4−S128
Y99F (90 μM)		15 276	15 251	V2−L134
		15 718	15 743	G4−G141
Y99F (20 mM)		15 714	15 743	G4−G141
		15 922	15 955	V2−G141

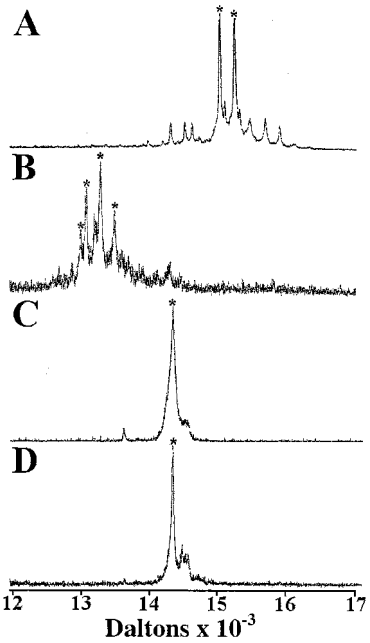

FIGURE 7: MALDI-TOF spectra of the α-core fragments generated by subtilisin digestion of CRP. The reaction conditions were (A) WT CRP and 90 μM cAMP; (B) Y99A CRP and 90 μM cAMP; (D) Y99A CRP and 20 mM cAMP; (D) Y99A/T127C CRP and 90 μM cAMP. The Y99A/T127C CRP was estimated, based on its behavior in SDS·PAGE, to be greater than 80% cross-linked through an intersubunit disulfide bond. Asterisks indicate the mass peaks included in Table 3.

sequence, VLGLPQTD, is that predicted for CRP after removal of the N-terminal formylmethionine (*3*, *4*). Removal of the N-terminal formylmethionine and the residues V1 and L2 generated the second sequence, GLPQTD. Precise CRP core fragment masses were determined from MALDI-TOF mass spectra for selected CRP core populations (Figure 7, Table 3). This information, coupled with the N-terminal sequence data, was used to deduce the C-terminal amino acid residue for each CRP core fragment population (Table 3).

Protease digestion reactions that contained WT CRP and 90 μM cAMP produced core fragments that terminated at position 134 located in the hinge region that connects the C- and N-proximal domains of CRP (Figures 1 and 7, Table 3). Similarly, subtilisin produced core fragments from Y99F CRP in the presence of either 90 μM or 20 mM cAMP that terminated at amino acid residues L134 through A141. The Y99A CRP in the presence of 90 μM cAMP [i.e., CRP:$(cAMP)_1$] produced a population of core fragments that terminated at amino acid residues L116−A121, C-helix residues located at the subunit interface in dimer CRP (Figures 1 and 7, Table 3). The production of low-mass core fragments from Y99A CRP may have resulted from alanine substitution affecting a CRP hinge conformation change. Following this reasoning, a hinge-region peptide bond would serve as the initial substrate for subtilisin to yield a high-mass core that was subsequently degraded to a low-mass core. The results of two experiments are not consistent with this interpretation. First, time-course subtilisin digestion reactions failed to reveal the high-mass core intermediate expected if CRP hinge cleavage were to precede protease cleavage of C-helix residues (data not shown). In contrast, digestion of the Y99A CRP in the presence of 90 μM cAMP does proceed through a transient high mass α-core fragment, indicating that, when bound by cAMP, the Y99A CRP hinge is protease sensitive (data not shown). Second, the Y99A/T127C apo-CRP, having subunits cross-linked by a disulfide bond at position 127, was resistant to subtilisin (data not shown). Clearly, neither the Y99A/T127C CRP hinge-region peptide bonds nor subunit interface C-helix peptide bonds were accessible to the protease. These results lead us to favor an alternative interpretation regarding the basis for Y99A apo-CRP sensitivity to subtilisin: Y99A affects not the CRP hinge conformation per se but rather destabilizes the CRP dimer to allow protease access to buried subunit interface amino acid residues. We have found that increasing the cAMP concentration from 90 μM to 20 mM, a condition known to strengthen intersubunit interactions (*7*), resulted in the production of high-mass Y99A CRP core fragments that terminated at S128, a residue located near the CRP hinge (Figure 7, Table 3). In addition, the disulfide cross-linked T127C/Y99A CRP produced, in the presence of 90 μM cAMP, a core fragment that terminated at S128 when incubated with protease (Figure 7, Table 3). These last two observations are consistent with the hypothesis that Y99A affects CRP dimer stability. To test this, we have assayed the rates of CRP subunit exchange for the WT and position 99 mutant forms of CRP.

The subunit exchange assay developed for the current study was adapted from the assay protocol originally described by Brown and Crothers (*7*). Our exchange assay utilizes two populations of CRP, one of which contains an N-terminal protein kinase recognition sequence and one of which contains both the protein kinase recognition sequence and a C-terminal hexahistidine sequence (*14*). The assay is conducted in three stages. First, radiolabled MVRRASV-CRP-RS was diluted and the monomer/dimer distribution allowed to equilibrate. Second, a 9-fold molar excess of unlabeled, MVRRASV-CRP-RSH_6 was added to establish a heterodimer pool whose rate of formation would reflect the rate of subunit exchange. Third, the CRP heterodimer population, composed of one hexahistidine-tagged and one radiolabeled subunit, was separated from radiolabeled homodimer over time on a Ni-chelating column. Three lines of evidence indicate that use of MVRRASV-CRP-RSH_6 in studying CRP subunit exchange is valid. First, the MVRRASV-CRP-RSH_6 and WT CRP show similar characteristics in cAMP and DNA binding (*14*). Consistent with

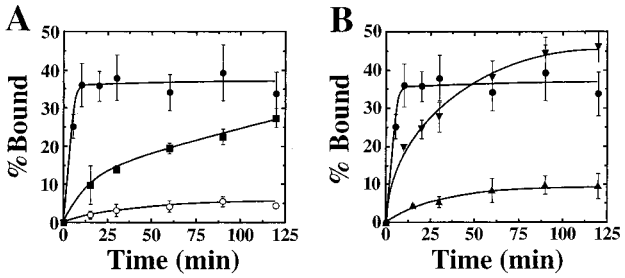

FIGURE 8: (A) CRP subunit exchange for the apo-forms of WT CRP (open circles), Y99A CRP (closed circles) and Y99F CRP (closed squares). The data are expressed as the amount of labeled CRP subunit bound to a Ni-chelating column expressed as a percent of the total labeled subunit in the reaction mixture versus time. At 24 h, the level of exchange was for WT CRP, 22%; for Y99A CRP, 33%; and for Y99F CRP, 35%. (B) Subunit exchange for the apo-form of Y99A CRP (closed circles), Y99A CRP in the presence of 90 μM cAMP (inverted triangles), and Y99A CRP in the presence of 2 mM cAMP (triangles). At 24 h, the level of exchange was for Y99A CRP, 33%; for Y99A CRP and 90 μM cAMP, 42%; and for Y99A CRP and 2 mM cAMP, 15%.

this we have observed that *E. coli* 8445 cells that contain MVRRASV-CRP-RSH_6 display a wild-type phenotype when cultured in the presence of cAMP indicating that MVRRASV-CRP-RSH_6 and RNAP interact productively (data not shown). Second, after incubation at 37 °C for 24 h, 40−45% of the label contained in MVRRASV-CRP-RSH_6/radiolabled MVRRASV-CRP-RS mixtures bound to a Ni-chelating column; this level of binding approaches the theoretical maximum of 50%. Third, time course studies show that radiolabled MVRRASV-CRP-RS subunits exchange with a half time of ~5 h (data not shown), results consistent with those reported for WT CRP (*7*). More detailed characterization of the subunit assay is beyond the scope of this study and will be presented elsewhere.

For the present study, we chose to monitor CRP subunit exchange under conditions that approximate the temperature and buffer conditions the protease digestion assay. At 26 °C, WT CRP subunits showed a progressive, time-dependent exchange that reached a maximum of 5% exchange over a 2 h period (Figure 8A). This contrasts with the subunit exchange characteristics of both the Y99F and the Y99A CRP which, over the 2 h time course showed 27 and 37% exchange, respectively. The Y99F showed a progressive, time-dependent increase in heterodimer formation over the 2-h incubation period whereas the Y99A CRP subunit exchange was complete in 10 min. Clearly, these results show that amino acid substitution at position 99 affects the rate at which CRP subunits exchange. The results of the subunit exchange assay confirm directly the hypothesis that Y99A amino acid substitution destabilizes the apo-CRP dimer. The results of Y99A CRP proteolysis suggested that high concentrations of cAMP stabilized the Y99A dimer. Indeed, the results presented in Figure 8B show that at 90 μM cAMP slowed the rate of Y99A CRP subunit exchange by a factor of 5. At 2 mM, cAMP radically slowed the subunit exchange rate close to that observed for WT apo-CRP.

DISCUSSION

The characteristics of Y99F and Y99A CRP are similar to those of WT CRP. All three forms of CRP are dependent upon cAMP to activate *lac* mRNA synthesis both in vivo

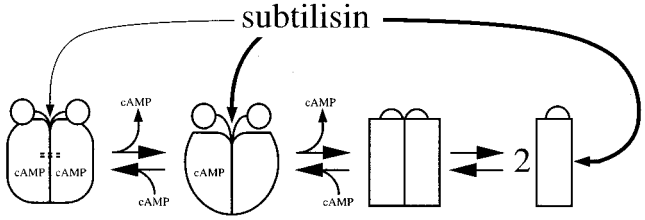

FIGURE 9: Schematic representation of the interaction of CRP and subtilisin.

(Figure 2) and in vitro (Figure 5). All three forms of CRP have similar affinity for cAMP, and all exhibit negative cooperativity in cAMP binding (Figure 3, Table 2). All bind *lac*P DNA with high affinity in the presence of cAMP (Figure 4, Table 2) and stimulate the formation of CRP:cAMP:RNAP complexes at *lac*P that yield equivalent levels of *lac* mRNA in vitro (Figure 5). Despite these similarities, a major difference in subunit interactions exists between the WT CRP and the position 99 amino acid substituted forms of CRP.

Conclusion 1. Amino Acid Substitution at Position 99 Destabilizes CRP Subunit Association. CRP structure changes occur as the result of cAMP binding. One hallmark difference between apo-CRP and the CRP:cAMP complex is hinge-region susceptibility to protease (*1*, *6*, *9*, *21*, *30*, *32*). Apo-CRP is protease resistant. In the presence of cAMP, subtilisin cleaves WT CRP to a heterogeneous population of α-core fragments. These core fragments share a common N-terminal amino acid sequence and, depending on the reaction conditions, have C-termini between amino acid residues 116 and 141 (*30*, *32*). Under the conditions utilized in our study, the WT apo-CRP and Y99F apo-CRP were found to be protease resistant. In contrast, the Y99A apo-CRP was protease sensitive (Figure 6). Y99A apo-CRP protease sensitivity is not the result of structure changes in Y99A CRP hinge conformation. There is no evidence to suggest that at early incubation times a short-lived high-mass core fragment is produced from Y99A CRP by subtilisin, an expected result if indeed proteolysis was initiated at the hinge. In addition, the apo-form of T127C/Y99A CRP, having subunits cross-linked through a disulfide bond, was protease resistant.

Subtilisin produced from the WT CRP:$cAMP_1$ and Y99F CRP:$cAMP_1$ complexes high-mass core fragments that terminated in the CRP hinge region. In contrast, subtilisin produced from the Y99A CRP:$cAMP_1$ low-mass core fragments that had C-termini that mapped to dimer interface residues (Table 3). The results of CRP subunit exchange experiments provide a clear basis for understanding how subtilisin gained access to C-helix residues buried at the interface of CRP subunits in the Y99A CRP dimer; the Y99A CRP subunit exchange rate is much greater than that observed for WT CRP. The end result of increased exchange rate is increased C-helix residue exposure to solvent and hence to protease. A schematic representation of the proteolysis characteristics of CRP is shown in Figure 9. We envision that two regions exist in CRP that may serve as the initial substrate for protease. The first is located in the hinge. Protease access to CRP hinge-region peptide bonds requires the conformation change induced by cAMP binding. At a cAMP concentration sufficiently high to promote the formation of CRP:$(cAMP)_2$, protease access to the hinge is limited. The second initial substrate for subtilisin is located

in the CRP C-helix. Protease access to C-helix peptide bonds requires subunit dissociation.

The rates of subunit exchange for the three forms of CRP rank, from greatest to least, Y99A CRP ≫ Y99F CRP > WT CRP. WT CRP, at 37 °C, has a subunit association constant on the order of 10^9-10^{10} M^{-1} with a half-time of 5 h. (*7*). Consequently, at 26 °C we observed little WT CRP subunit exchange, and hence, little C-helix exposure in the 1 h incubation with protease. This was not the case for the Y99A CRP, where the rate of subunit exchange was sufficiently high to allow, over 1 h, extensive C-helix exposure to protease. The Y99F CRP, while displaying a subunit exchange rate intermediate to those of the WT CRP and Y99A CRP, did not produce measurable amounts of the low-mass core fragment.

Conclusion 2. Tyrosine at Position 99 Anchors the CRP B-Helix to the CRP Surface. Both the tyrosine hydroxyl group and aromatic ring contribute to Y99 stabilizing CRP subunit interactions. The buried tyrosine aromatic ring, it appears, provides stability by anchoring the CRP B-helix to the protein surface (Figure 1C). Eliminating this tyrosine B-helix anchor by replacing tyrosine with alanine is likely to increase B-helix mobility in three dimensions and results in a large increase in the rate of CRP subunit exchange.

Eliminating the tyrosine hydroxyl group by replacement with phenylalanine produced a small increase in the rate of CRP subunit exchange. The origin of this contribution is less certain. Weber and Steitz (*5*) predicted that Y99 plays a role in stabilizing the cAMP binding pocket through hydrogen-bonding interactions with the carbonyl group of G71 and a guanidinium nitrogen of R82. Eliminating the potential for these hydrogen-bonding interactions while maintaining an aromatic ring structure at position 99 may increase B-helix mobility in only one dimension and result in a small increase in the rate of CRP subunit exchange.

Baichoo and Heyduk (*14*, *15*) provided evidence that the position of the B-helix changes during the course of ligand binding. In the absence of cAMP, the CRP B-helix peptide bonds are protected from low-mass chemical proteases. In the presence of cAMP, the CRP B-helix is more solvent exposed and shows hypersensitivity to $[(OP)_2Cu]^+$. Similarly, the structural organization of the N- and C-proximal ends of the C-helix and the entire B-helix changes in response to CRP:cAMP complex binding to DNA as evidenced by the relatively large change in B-helix peptide bond sensitivity to $[(OP)_2Cu]^+$ (*15*). It is tempting to speculate that surface position changes in the B-helix arise directly from tyrosine 99 interaction with cAMP and promote positional changes in, for example, the CRP C-helix. It is equally likely, however, that B-helix motions occur in response to more generalized structure changes. If this is the case, then it follows that Y99 anchors the B-helix to the surface of the protein and provides a point against which ligand-induced B-helix motions may be used to mediate, for example, motions in the C-helix and thereby affect CRP subunit interactions.

Conclusion 3. CRP:$(cAMP)_1$ and CRP:$(cAMP)_2$ Have Different Rates of CRP Subunit Exchange. Brown and Crothers (*7*) showed that cAMP stabilizes CRP subunit association; at a concentration of 85 μM, cAMP decreased the rate of CRP subunit exchange by a factor of 4. Similarly, we show here that at a concentration of 90 μM, cAMP decreased the rate of Y99A CRP subunit exchange by a factor of 5. We note that at these cAMP concentrations the CRP population is >95% CRP:$(cAMP)_1$. Brown and Crothers (*7*) concluded that cAMP-mediated subunit stabilization was mediated through hydrogen bonding between cAMP bound to one subunit with S128 located on the opposite subunit. Won et al. (*16*) have recently published information that provides an alternative means of stabilizing CRP subunit interactions. There appears to be a significant difference between the apo-CRP and CRP:$(cAMP)_2$ hinge regions. For CRP:$(cAMP)_2$, the residues that define the C-terminal portion of the cAMP binding domain and the N-terminal portion of the DNA binding domain extend from 110−133 (C-helix) through 134−138 (hinge) to 139−148 (D-helix) (Figure 1). In contrast, apo-CRP residues 127−133 appear not to participate in forming α-helical structure whereas residues 134−139 do. This suggests that one consequence of cAMP binding to apo-CRP is to change the secondary structure of the region including residues 127−139, effectively translating the flexible hinge six residues toward the CRP C-proximal domain. Such a conformation change would increase the length of the C-helix by 26%, increase the overall surface area available for CRP subunit interaction, and decrease the rate of CRP subunit exchange.

The results of our study also show that at a cAMP concentration sufficiently high to promote formation of CRP:$(cAMP)_2$ the Y99A CRP subunits exchanged at a rate >150-fold slower than that measured for Y99A apo-CRP, showing only 15% exchange over a period of 24 h. At 2 mM cAMP the CRP population is calculated to be 56% CRP:$(cAMP)_1$ and 44% CRP:$(cAMP)_2$. We conclude from this that the 2:1 binding of cAMP to Y99A CRP provided a greater stabilizing effect on CRP subunit association than did the 1:1 binding of cAMP to Y99A CRP. Since the potential to form as many as four hydogen bonds between cAMP and S128 exists in CRP:$(cAMP)_2$, we predict that, in addition to increased subunit surface area, intersubunit hydrogen bonding plays a major role in stabilizing CRP:$(cAMP)_2$ subunit association.

If the Y99 hydroxyl were important in CRP binding cAMP we expected to observe *decreased* cAMP affinity for both the Y99F CRP and the Y99A CRP. We found instead that eliminating the tyrosine hydroxyl group produced a modest 2−3-fold *increase* in CRP affinity for cAMP (Table 2). Clearly, tyrosine 99 does not play a direct role in cAMP binding by contributing to the binding energy. If, as suggested by Weber and Steitz (*4*), the cAMP pocket is stabilized by Y99, the Y99 tyrosine hydroxyl determines, in part, the overall structure and rigidity of a ligand binding pocket that has a defined affinity for cAMP. Removal of the hydroxyl group may introduce flexibility to the cAMP binding pocket and produce a modest increase in CRP affinity for the ligand.

In summary, this study was undertaken to test the hypothesis, developed from molecular modeling, that Y99 interacts with cAMP in the CRP:cAMP complex. We have no experimental evidence to support such an interaction. We have, however, established that the amino acid residue at position 99 plays an important role in determining the rates at which CRP subunits exchange. The Y99 aromatic ring appears to anchor the CRP B-helix to the surface of the protein. Removing the Y99 hydroxyl group or the aromatic ring increases the rate at which CRP subunits exchange but

has little effect on CRP function in cAMP or DNA binding or on CRP-mediated activation of *lac*P. Our analysis of the position 99 mutant forms of CRP leads us to conclude that, in CRP, two substrates for subtilisin exist: hinge region peptide bonds, and C-helix peptide bonds (Figure 9). CRP protease sensitivity has been used as a diagnostic tool to monitor changes in CRP structure. This study shows that care must be taken in interpreting protease digestion results. One must distinguish the effects of effector binding or amino acid substitution (i.e., CRP*, ref *1*) on CRP hinge conformation that leads to protease cleavage of hinge-region peptide bonds from protease cleavage of C-helix peptide bonds that results from increased rates of CRP subunit exchange.

ACKNOWLEDGMENT

We are grateful to Tomasz Heyduk for providing *E. coli* strain M15/pREP4 and pQE60NB1 encoding MVRRASV-CRP-RSH_6 CRP and to George Makhatadze and Marimar Lopez for useful discussions on conducting the fluorescence titration measurements. We also thank Susan San Francisco for synthesizing oligonucleotides and performing the N-terminal amino acid sequence analysis of CRP α-core fragments and Sew-Fen Leu for conducting the DNase I footprint reactions.

REFERENCES

1. Harman, J. G. (2001) *Biochim. Biophys. Acta 1547*, 1−17.
2. Aiba, H., Fujimoto, S., and Ozaki, N. (1982) *Nucleic Acids Res. 10*, 1345−1362.
3. Cossart, P., and Gicquel-Sanzey B. (1982) *Nucleic Acids Res. 10*, 1363−1378.
4. Weber, I. T., and Steitz, T. A. (1987) *J. Mol. Biol. 198*, 311−326.
5. Takahashi, M., Blazy, B., Baudras, A., and Hillen, W. (1989) *J. Mol. Biol. 207*, 783−796.
6. Heyduk, T., and Lee, J. C. (1989) *Biochemistry 28*, 6914−6924.
7. Brown, A. M., and Crothers, D. M. (1989) *Proc. Natl. Acad. Sci. U.S.A. 86*, 7387−7391.
8. Cheng, X., Gonzalez, M. L., and Lee, J. C. (1993) *Biochemistry 32*, 8130−1839.
9. Eilen, E., Pampeno, C., and Krakow, J. S. (1978) *Biochemistry 17*, 2469−2473.
10. Ebright, R. H., Ebright, Y. W., and Gunasekera, A. (1989) *Nucleic Acids Res. 17*, 10295−10305.
11. Heyduk, T., Lee, J. C., Ebright, Y. W., Blatter, E. E., Zhou, Y., and Ebright, R. H. (1993) *Nature 364*, 548−549.
12. Busby, S., and Ebright, R. H. (1999) *J. Mol. Biol. 293*, 199−213.
13. Passner, J. M., Schultz, S. C., and Steitz, T. A. (2000) *J. Mol. Biol. 304*, 847−859.
14. Baichoo, N., and Heyduk, T. (1997) *Biochemistry 36*, 10830−10836.
15. Baichoo, N., and Heyduk, T. (1999) *Protein Sci. 8*, 518−528.
16. Won, H.-S., Yamazaki, T., Lee, T.-W., Yoon, M.-K., Park, S.-H., Otomo, T., Kyogoku, Y., and Lee, B.-J. (2000) *Biochemistry 39*, 13953−13962.
17. Garcia, A. E., and Harman, J. G. (1996) *Protein Sci. 5*, 62−71.
18. Passner, J. M., and Steitz, T. A. (1997) *Proc. Natl. Acad. Sci. U.S.A. 94*, 2843−2847.
19. García, A. E. (1992) *Phys. Rev. Lett. 68*, 2696−2699.
20. Garcia, A. E., Blumenfeld, R., Hummer, G., and Krumhansl, J. A. (1997) *Physica D 107*, 225−239.
21. Harman, J. G., Peterkofsky, A., and McKenney, K. (1986) *J. Biol. Chem. 261*, 16332−16339.
22. Zuber, M., Patterson, T. A., and Court, D. L. (1987) *Proc. Natl. Acad. Sci. U.S.A. 84*, 4514−4518.
23. Bernard, H.-U., and Helinski, D. R. (1979) *Methods Enzymol. 68*, 482−493.
24. Belduz, A. O., Lee, E. J., and Harman, J. G. (1993) *Nucleic Acids Res. 21*, 1827−1835.
25. Kunkel, T. A. (1985) *Proc. Natl. Acad. Sci.U.S.A. 82*, 488−492.
26. Miller, J. H. (1972) *Experiments in Molecular Genetics*, Cold Spring Harbor Laboratory Press, Cold Spring Harbor, NY.
27. Burgess, R. R., and Jendrisak, J. J. (1975) *Biochemistry 14*, 4634−4638.
28. Lowe, P. A., Hager, D. A., and Burgess, R. R. (1979) *Biochemistry 18*, 1344−1352.
29. Leu, S.-F., Baker, C. H., Lee, E. J, and Harman, J. G. (1999) *Biochemistry 38*, 6222−6230.
30. Tsugita, A., Blazy, B., Takahashi, M., and Baudras, A. (1982) FEBS *Lett. 144*, 304−308.
31. Chen, Y., Ebright, Y. W., and Ebright, R. H. (1994) *Science 265*, 90−92.
32. Lee, E. J., Glasgow, J., Leu, S.-F., Belduz, A. O., and Harman, J. G. (1994) *Nucleic Acids Res. 22*, 2894−2901.

BI010834+